Published in final edited form as:
Mol Cell Neurosci. 2011 January ; 46(1): 347–356. doi:10.1016/j.mcn.2010.11.003.

Midbrain dopaminergic axons are guided longitudinally through the diencephalon by Slit/Robo signals

James P Dugan, **Andrea Stratton**, **Hilary P Riley**, **W Todd Farmer**, and **Grant S Mastick***
Department of Biology, University of Nevada, Reno, NV 89557

Abstract

Dopaminergic neurons from the ventral mesencephalon/diencephalon (mesodiencephalon) form vital pathways constituting the majority of the brain's dopamine systems. Mesodiencephalic dopaminergic (mdDA) neurons extend longitudinal projections anteriorly through the diencephalon, ascending toward forebrain targets. The mechanisms by which mdDA axons initially navigate through the diencephalon are poorly understood. Recently the Slit family of secreted axon guidance proteins, and their Robo receptors, have been identified as important guides for descending longitudinal axons. To test the potential roles of Slit/Robo guidance in ascending trajectories, we examined tyrosine hydroxylase-positive (TH+) projections from mdDA neurons in mutant mouse embryos. We found that mdDA axons grow out of and parallel to Slit-positive ventral regions within the diencephalon, and that subsets of the mdDA axons likely express Robo1 and possibly also Robo2. Slit2 was able to directly inhibit TH axon outgrowth in explant co-culture assays. The mdDA axons made significant pathfinding errors in *Slit1/2* and *Robo1/2* knockout mice, including spreading out in the diencephalon to form a wider tract. The wider tract resulted from a combination of invasion of the ventral midline, consistent with Slit repulsion, but also axons wandering dorsally, away from the ventral midline. Aberrant dorsal trajectories were prominent in *Robo1* and *Robo1/2* knockout mice, suggesting that an aspect of Robo receptor function is Slit-independent. These results indicate that Slit/Robo signaling is critical during the initial establishment of dopaminergic pathways, with roles in the dorsoventral positioning and precise pathfinding of these ascending longitudinal axons.

Keywords

Slit; Robo; Dopaminergic; Longitudinal; Axon guidance

*Correspondence to: Grant S. Mastick, Department of Biology, University of Nevada, 1664 N. Virginia St., Reno, NV 89557. gmastick@unr.edu, Telephone: 775-784-6168.

Authors' contributions:
JPD participated in the design of the study, carried out embryo labels and analysis, carried out explant analysis, and drafted the manuscript. AS participated in the immunohistology to localize Robo expression. HPR participated in embryo labels and analysis. WTF contributed in situ hybridization analysis of Slit expression. GSM participated in the design of the study, participated in embryo labels and analysis, and drafted and revised the manuscript.

Competing interests: The authors declare that they have no competing interests.

1. Introduction

Ventral mesodiencephalic dopaminergic (mdDA) axons form the major dopamine-containing pathways in the brain, and are affected in several disorders. Parkinson's disease results from the degeneration of the nigrostriatal fibers that connect the substantia nigra pars compacta (SNc) to the striatum (Poirier and Sourkes, 1965; Savitt et al., 2006). In the mesolimbic pathway, formed between the ventral tegmental area (VTA) and nucleus accumbens, disruption of dopamine signaling has been linked to symptoms of schizophrenia (Sesack and Carr, 2002). Although these tracts have been extensively studied in the context of disease, the embryonic development of mdDA axonal projections has only recently been explored.

During early development, mdDA axons traverse the diencephalon in a tight longitudinal pathway. They first project anteriorly at a narrowly defined lateral position, specifically avoid projections into dorsal or ventral regions, and exit the diencephalon into the telencephalon at a specific point (Hu et al., 2004; Voorn et al., 1988). These trajectories are relatively simple and early, and so represent an important example of ascending longitudinal projections.

Mechanisms that guide aspects of the mdDA tract have begun to be defined in several recent studies. The anterior direction of projections is the result of directional cues within the substrate, as shown by surgical rotations in cultured ventral diencephalon tissue (Nakamura et al., 2000). These directional cues appear to include repellent Semaphorin signals, because several Semas are expressed in diencephalic and adjoining tissues, and can regulate outgrowth of cultured mdDA axons (Hernandez-Montiel et al., 2008; Kolk et al., 2009; Torre et al., 2010; Yamauchi et al., 2009). Furthermore, mutations in the Sema receptor Neuropilin2 cause a subset of mdDA axons to project posteriorly instead of anteriorly (Yamauchi et al., 2009). Once the axons start growing anteriorly, several molecular cues are expressed in the diencephalon, including both repellents and attractants with potential roles in defining the narrow tract. Directed mdDA axon growth is dependent on regional specification and patterning within the diencephalon, as implied by mdDA errors in mice mutant for the transcription factor Pax6, possibly mediated by altered expression patterns of the midline attractant Netrin1 (Vitalis et al., 2000). Netrin1 can attract mdDA axons in culture (Lin et al., 2005). Sema/Npn2 repulsion is again involved, because a subset of mdDA axons spread dorsally from the main tract in Npn2 mutants, implicating a broad lateral arc of Sema in channeling mdDA axons anteriorly (Kolk et al., 2009; Yamauchi et al., 2009). Further along the mdDA pathway, the morphogen Shh contributes to setting the position of the anterior tract, in that Shh acts as an attractant for mdDA axons in vitro, and receptor-blocking mutations cause a subset of axons to make errors near the telencephalon entry point (Hammond et al., 2009). However, for many of the molecular cues identified to date, in vivo roles remain to be fully defined, and likely other cues are involved.

The Slit family of chemorepulsive molecules plays important roles in many axonal trajectories (reviewed in Dickson and Gilestro, 2006). The Slits operate via their main receptors, the Robos. In the mammalian brain, three Slits (Slit1, Slit2, Slit3) have been identified, as well as three Robos (Robo1, Robo2, Robo3/Rig1). Recent studies have shown that Slit/Robo signaling is necessary for longitudinal axon guidance. Within descending longitudinal projections, Slit/Robo signaling provides cues for defining dorsoventral topology and preventing axons from entering the floor plate (Devine and Key, 2008; Farmer et al., 2008; Kastenhuber et al., 2009). In the medial longitudinal fasciculus (MLF), a descending longitudinal population extending from the midbrain through the hindbrain, Slit/Robo signaling prevents axons from entering the ventral midline tissue of the floor plate, and also promotes straight longitudinal growth (Farmer et al., 2008). Given the importance

of Slit/Robo signaling in guiding descending axons, the ipsilateral ascending trajectories of the mdDA axons may also depend on Slit/Robo signaling. Consistent with this, Slit2 repels mdDA neurons in vitro (Lin et al., 2005). In *Slit1/2* double mutant mice, at late stages of fetal development (embryonic day 18, E18) by which time the tract is normally complete, the tract has a disrupted organization, with TH+ bundles near the ventral midline in the diencephalon, a Slit+ region that they normally avoid (Bagri et al., 2002). These observations suggest that Slit/Robo signaling has roles in vivo in guiding mdDA axons.

In this study, we set out to better define the role of Slit/Robo signals in guiding mdDA axon trajectories, by focusing on the initial stages of mdDA outgrowth as the first pioneer axons establish the tract through the diencephalon. The specific goals of the study were to determine whether the pioneer axons were in position to be influenced by Slit/Robo signals, whether they could directly respond to Slits, and whether Slit/Robo signals were required in vivo to guide their trajectories.

2. Materials and Methods

Animals

Mice procedures were reviewed by the UNR IACUC protocol, following NIH guidelines. Expression data was performed using CD-1 wild-type embryos. E12.5 and E13.5 mutant embryos were obtained via uterine dissection by mating *Robo1*$^{+/-}$, *Robo2*$^{+/-}$, *Robo1*$^{+/-}$; *Robo2*$^{+/-}$, *Slit1*$^{-/-;}$ *Slit2*$^{+/-}$, or *Slit1*$^{+/-;}$ *Slit2*$^{+/-}$ mice, which were maintained in a CD1 background. The mutant founder lines were a gift of Marc Tessier-Lavigne, Genentech. PCR genotyping was performed as previously described (Grieshammer et al., 2004; Long et al., 2004; Plump et al., 2002). For each genotype, 3-6 embryos were analyzed, as indicated in the Results text, and mutant phenotypes were consistent within each genotype.

In Situ Hybridization

Whole-mount in situ hybridization was carried out as previously described (Mastick et al., 1997). Probes for rSlit1, rSlit2, rSlit3, rRobo1 and rRobo2 were provided by Marc Tessier-Lavigne, Genentech.

Immunofluorescence on sections

E12.5 embryos were sectioned at 20 μm using a cryostat (Leica). Sections were interleaved on Superfrost slides (Fisher). Robo1 and 2 antibodies were obtained from Elke Stein (Yale), using a C-terminal 100 amino acid segment of the mouse proteins as antigens in rabbit (1:800 dilution). β-gal (rabbit, Cappel, 1:1000 dilution) and TH (rabbit, Pel-Freez, 1:500 dilution) primary antibodies were also used. Slides were blocked in slacker solution (PBS, 5% fetal bovine serum, 0.1% Triton X-100) for 1 hr, incubated overnight in primary antibody diluted in the blocking solution, washed 3 times for 15 min, incubated for 1 hr in secondary antibody (JacksonImmunoResearch, 1:200 dilution), washed 3 times for 15 min, and coverslip-mounted using FluorSave (Calbiochem). As the TH and Robo1 antibodies were both produced in rabbit, double labeling was carried out using an anti-rabbit Fab secondary antibody (Negoescu et al., 1994). Anti-TH primary antibody was applied first, followed by an anti-rabbit DyLight 488 Fab fragment (Jackson ImmunoResearch), and an incubation for two hours with an anti-rabbit unconjugated Fab fragment to bind to any remaining epitopes on the TH primary antibody. A second round of antibody labeling then used a Robo primary antibody, followed by anti-rabbit Alexa 555 polyclonal secondary antibody. A control labeling was done in parallel, omitting the second primary antibody, which showed that the red secondary antibody had little reaction to the first primary antibody.

Immunofluorescence on whole mounts

For whole-mount immunolabeling, embryos were fixed in 4% PFA overnight. Skin and mesenchyme were dissected away from the brain and the brains were bisected along the ventral and dorsal midlines. The technique using TH (1:500) and Cy3-conjugated secondary antibody (Jackson ImmunoResearch, 1:200 dilution) was as previously described (Nural and Mastick, 2004). Imaging of the whole mounts was done at low magnification with a Leica DM5000 epifluorescence microscope, and at high magnification with an Olympus confocal microscope. Quantitative analysis of the tract widths was done on different combination of Slit genotypes, using ImageJ to measure the width of the tracts by an observer blinded to the genotypes.

Preparation of cell aggregates expressing Slit2

Transfection of *Slit2* into COS-7 cells was performed using Lipofectamine (Invitrogen) as directed. COS cell aggregates were prepared as previously described (Kennedy et al., 1994), except cells were resuspended in collagen, placed on lids, and inverted over media (95% DMEM, 5% FBS) for three hours to prepare hanging drop aggregates.

Explant culture preparation

Explant preparation was performed as previously described (Lin et al., 2005). In brief, tissue from the ventral midbrain (VM) was removed from E12.5 embryos. The ventral midbrain was dissected and cut into small squares in L15 medium. The small squares were removed from the medium and placed into a single well of a 4-well plate using a mouth pipetter. A 20μl collagen bed was placed on the bottom of each well and a 20ul top layer was used to position the explanted tissue around the COS cell aggregates. Growth medium (50% F12/40% optimem/10% fetal calf serum/1X pen-strep/1X glutamax) was added to the well and explants were allowed to grow for 48 hours. After fixation, explants and cell aggregates were immunolabeled using standard technique (Lin et al., 2005; Sang et al., 2002). Aggregates transfected with *Slit2* were labeled to verify Slit2 expression with mouse anti-c-myc (Santa Cruz Biotechnology, 1:200 dilution) and Cy2-conjugated secondary antibody (1:200). Explanted tissue was labeled with rabbit anti-TH (1:500) and mouse anti-βIII tubulin (Covance, 1:1000) and Cy3- and Cy2-conjugated secondary antibodies (1:200), respectively.

Quantitative and statistical analyses of explants

Images of VM explants were marked into four quadrants with Adobe Illustrator CS3 (2007). The two quadrants used for quantification were designated proximal (P) and distal (D) with relation to the COS cell aggregates. Total number of axons and the lengths of the five longest axons in the distal quadrant and up to five axons in the proximal quadrant were measured using ImageJ (Meijering et al., 2004), by an independent observer in a double-blind strategy. P/D ratios were compared using Student's t-test. P values < 0.05 were considered significant.

3. Results

3.1. Initial outgrowth of mdDA axons is associated with Slit and Robo expression

The initial stages of mdDA axon trajectories are ideally visualized by TH antibody labels of whole mount embryos on E12. This approach provides a clear view of the initial trajectories of TH axons as they exit their nucleus, and turn anteriorly to traverse through the diencephalon (Fig 1A,B). mdDA projections are constrained along a narrow corridor at a specific dorsoventral position across the diencephalon and approach the telencephalon. The dopaminergic neurons of the A13 population serve as a landmark, as the mdDA axons grow

past the ventral side of the A13 enroute to the diencephalon/telencephalon border at E12.5 (Fig.1A,B). We will refer the normal position of the tract as the Medial Forebrain Bundle (MFB), in which the mdDA axons may be the first to ascend. The mdDA tract likely consists of a mixed population of TH+ SNc and VTA fibers, because, although there are no molecular markers available to distinguish between the two classes of fibers, their initial terminal arbors are extensively intermingled in the basal telencephalon based on retrograde labeling (Hu et al., 2004).

To determine if Slits and Robos were expressed at the right time and location to influence mdDA axons, we first analyzed wild-type expression of *Slit1*, *2* and *3* and *Robo1* and *2* at E12.5. Although *Slit* and *Robo* expression in the embryonic midbrain and diencephalon were described in previous studies at earlier and later stages (Bagri et al., 2002; Lopez-Bendito et al., 2007; Nural et al., 2007), expression patterns during initial outgrowth of mdDA axons remained unknown. *Slit1* and *2* mRNA patterns were examined by in situ hybridization. At E12.5, *Slit1* and *Slit2* expression were prominent at the ventral midline into the ventral midbrain (n = 10 of each). Much of their expression overlapped in the ventral midbrain, with *Slit1* extending farther dorsally than *Slit2* (Fig. 1C,D). *Slit1* was also expressed in faint dorsal patches in the midbrain and ventral diencephalon (Fig. 1C). In agreement with previous findings (Yuan et al., 1999), *Slit3* was not expressed in the midbrain or forebrain (n=4; data not shown). Overall, *Slit1* and *2* were expressed ventrally in the origin of mdDA neurons, as well as adjacent to their axonal pathway, most prominently in ventral diencephalon.

To examine Robo expression in mdDA neurons, a combination of antibody and transgene markers were used on E12.5 sagittal sections (Fig. 1E-H). Robo1 antibody labeling showed an extensive array of longitudinal bundles transiting the ventral diencephalon, arising from sources which were distinct from and preceding the appearance of TH+ fibers. Within TH+ cell bodies and their initial axon segments, Robo1 and TH antibody labels had only a partial overlap (Fig. 1F-H). Some TH+ cell bodies and their initial axon segments were Robo1+, while others did not have detectable Robo1 labeling. Interestingly, some TH+ axons were closely associated with Robo1+ bundles, appearing to fasciculate with these bundles. However, the initial segments of other subsets of TH+ axons were clearly unlabeled by Robo1 antibodies and were not associated with Robo1+ bundles. The fact that only a subset of TH+ axons are Robo1+ leaves unclear if distinct subpopulations vary in whether they express Robo1, or if Robo1 might be expressed during specific times of TH+ axon differentiation. However, the strong and pervasive axon guidance defects shown below imply that Robo1 expression is wider across the mdDA neuron populations than suggested by the available detection methods.

To examine Robo2 expression, Robo2 antibody labeling showed expression that was less widespread, as Robo2 was predominantly in longitudinal axons located dorsal, anterior, or posterior to and non-overlapping with the mdDA TH+ population (Fig 1I). To further investigate Robo2 expression, we also examined embryos carrying a *Robo2* mutant allele containing an *IRES-tauLacZ* expression cassette (Grieshammer et al., 2004) as revealed by an antibody against β-galactosidase (Fig. 1J, K). Axonal β-gal labeling was seen in the MFB, and appeared to extensively overlap with TH+ MFB axons in adjacent cross-sections (n = 4). This observation suggests that Robo2 may be expressed in mdDA axons, but likely at lower levels than Robo1, which is consistent with the mutant phenotypes described below.

3.2. mdDA axon growth is inhibited in vitro by secreted Slit2

To determine if Slits can directly influence mdDA axon outgrowth, a collagen gel co-culture assay was used. COS cells were transfected with *Slit2* expression plasmids, then co-cultured in collagen gels with ventral midbrain tissue containing mdDA neurons during the stage of

their initial outgrowth at E12.5. Compared with mock-transfected control COS cells, Slit2-expressing COS cells significantly reduced the number and length of TH+ VM axons, with the strongest effects in the quadrant proximal to the aggregate (Fig. 2 D-E). These findings agree with previous explants of mdDA axons begun at E14, when many would have already reached the telencephalon (Lin et al., 2005). These explants suggest that early mdDA axons can respond directly to Slit signals.

3.3. Slits organize mdDA projections through the diencephalon, with Slit2 in a dominant role

To test the in vivo function of Slits in guiding mdDA axons through the diencephalon, we examined mdDA trajectories by TH antibody labeling of whole-mount embryos, including Slit and Robo mutants (Fig 1B). *Slit1*$^{-/-}$; *Slit2*$^{+/-}$ control embryos formed a narrow and organized tract indistinguishable from wild-type (n = 4) (compare Fig.1B to Fig. 3B). These accurate projections indicate that *Slit1* is dispensable if *Slit2*$^{+}$ alleles are present. In contrast, *Slit1*$^{-/-}$; *Slit2*$^{-/-}$ double mutants (n = 5) had diverging projections that formed a wide tract. Many axons projected into ventral diencephalon tissue, approaching and crossing the ventral midline (Fig 3E). In addition, some mdDA axons wandered dorsally, and few long projections advanced as far as the A13 landmark (Fig. 3D).

To test the specific function of *Slit2*, *Slit1*$^{+/+}$; *Slit2*$^{-/-}$ embryos were analyzed to compare their axon phenotype to double mutants and control embryos (Fig 3G-H). *Slit1*$^{+/+}$; *Slit2*$^{-/-}$ embryos (n = 3) had many axons enter the ventral midline. Few long axons could be seen along the MFB tract, thus sharing the major phenotypes of *Slit1*$^{-/-}$; *Slit2*$^{-/-}$ double mutants. Interestingly, the *Slit2*$^{-/-}$ single mutant phenotype appeared more organized than the *Slit1*$^{-/-}$; *Slit2*$^{-/-}$ double mutant, with few dorsal wandering trajectories, suggesting that Slit1 does contribute to mdDA guidance. To quantify the severity of TH+ axon errors between different Slit mutant genotypes, the width of the tract was measured (Fig 3M). This analysis showed that the homozygous loss of Slit2 caused a widening of the tract relative to Slit1 homozygous control embryos. The quantitation also confirmed that *Slit1*$^{-/-}$; *Slit2*$^{-/-}$ double mutants had a significantly wider tract than *Slit2*$^{-/-}$ single mutants, consistent with a Slit1 contribution to mdDA guidance, at least in the context of the *Slit2*$^{-/-}$ mutant background.

To examine whether the early mdDA errors result from a developmental delay in axon growth, or if the axons can recover from their errors, we also examined the tract a day later, on E13.5 (Fig 3J-L). *Slit1*$^{-/-}$; *Slit2*$^{-/-}$ double mutants (n = 3) showed an increase in axon projections through the diencephalon, suggesting that some axons eventually grew along the proper pathway. However, few axons reached the telencephalon, due to accumulating errors of several types: extensive broadening at the beginning of the tract, invasion of the ventral midline, and an accumulation of truncated axons near the A13 landmark. Strikingly, most axons that passed the A13 landmark veered anteriorly, approaching the optic chiasm (Fig 3K).

Overall, it appears that Slit2 is necessary for guidance of mdDA neurons into the MFB tract. A major role is to prevent aberrant axons from entering the ventral midline, consistent with ventral midline Slit expression. Additional and unexpected roles are to restrict mdDA axons to a narrow tract, and to prevent anterior projections toward the optic chiasm. Slit1 contributes a minor role in mdDA axon guidance.

3.4. Robos guide mdDA axons, in part through unique Robo1 and Slit-independent functions

Since Slits are the only known ligands for Robos, we examined mutants for *Robo1* and *Robo2*, singly (Fig 4) and combined (Fig 5), to test the prediction that these receptors mediate mdDA responses to Slits.

Robo2$^{-/-}$ embryos had wildtype mdDA projections, with a narrow tract and long projections along the expected path (n=3) (Fig. 4A). However, *Robo1*$^{-/-}$ homozygotes showed errors in mdDA projection patterns (n=6) (Fig. 4C-D). These errors included widening of the tract through the diencephalon, similar to *Slit1*$^{-/-}$; *Slit2*$^{-/-}$ double mutants. The widening resulted from many axons deviating both ventrally and dorsally from the normal MFB position. As in *Slit1*$^{-/-}$; *Slit2*$^{-/-}$ double mutants, many axons grew into ventral midline tissue. Other axons projected over the A13 landmark instead of traversing ventrally around it. Strikingly, *Robo1*$^{-/-}$ mutants formed a distinct ectopic bundle of axons that projected from the mdDA nucleus dorsally along the dorsal thalamus-pretectum boundary (Fig. 4D). Axons fasciculated and followed this narrow trajectory as far as the dorsal midline (presumptive epithalamus). This ectopic tract was not seen in *Slit1*$^{-/-}$; *Slit2*$^{-/-}$ double mutants.

Robo1$^{-/-}$; *Robo2*$^{-/-}$ double homozygotes (n = 4) had more severe phenotypes than *Robo1*$^{-/-}$ mutants, and were in several respects similar to *Slit1*$^{-/-}$; *Slit2*$^{-/-}$ double homozygotes. Specifically, mdDA axons looped ventrally to enter the ventral midline, wandered dorsally, formed a wider MFB, and were truncated, failing to make it beyond the A13 population (Fig. 5D,E). *Robo1*$^{-/-}$; *Robo2*$^{-/-}$ double homozygotes had the ectopic dorsal tract seen in *Robo1*$^{-/-}$ mutants (Fig. 5D). Overall, the *Robo1*$^{-/-}$; *Robo2*$^{-/-}$ double mutant phenotype appeared as severe as the *Slit1*$^{-/-}$; *Slit2*$^{-/-}$ double mutant phenotype. By E13.5, *Robo1*$^{-/-}$; *Robo2*$^{-/-}$ mutant embryos showed an expected increase in axonal projections, both within the MFB tract and into ectopic regions (n = 4) (Fig. 5G-J). As in *Slit1*$^{-/-}$; *Slit2*$^{-/-}$ double mutants, the beginning of the MFB tract was much wider, fasciculated into a very narrow bundle near A13, and many diverted off anteriorly toward the optic chiasm (Fig. 5G,I). Unique to *Robo1*$^{-/-}$; *Robo2*$^{-/-}$ double mutants, more axons projected dorsally from the mdDA nucleus, including some into dorsal midbrain (Fig. 5J). Overall, the *Robo1*$^{-/-}$; *Robo2*$^{-/-}$ double mutants have mdDA errors that partially overlapped with *Slit1/2* double mutant errors, but with increased severity and additional phenotypes.

4. Discussion

Slit/Robo signaling in commissural axon guidance has established the necessity of these molecules in organizing the early vertebrate brain (Bagri et al., 2002; Long et al., 2004). Recently, these same signaling molecules were shown to be important in the guidance of descending longitudinal axons that pioneer tracts in the brain (Devine and Key, 2008; Farmer et al., 2008; Kastenhuber et al., 2009). For axons descending through the embryonic mouse brain, a variety of roles have been implicated for Slit/Robo signaling including maintaining proper dorsoventral positioning, preventing ectopic projections into the ventral midline, and promoting straight axon growth (Farmer et al., 2008). Here we extend those findings to investigate the role of Slit/Robo signaling on a major longitudinal tract that is ascending.

The dopaminergic neurons of the ventral mesencephalon extend axons anteriorly through the presumptive diencephalon, continuing through to targets in the telencephalon. How these axons navigate along their initial trajectory from the ventral mesencephalon through the diencephalon is largely unknown. These longitudinal axons face the same challenges as other longitudinal populations. Unlike commissural axons that are guided by a distinct intermediate target like the ventral floor plate (Long et al., 2004; Tessier-Lavigne and

Goodman, 1996), longitudinal axons lack any obvious morphological features to follow, and do not share a common intermediate target. However, longitudinal axons run parallel to the ventral floor plate and may use secreted long range signals such as the Slits to set and maintain their dorsoventral position, and to prevent aberrant projections into the midline or other regions (Farmer et al., 2008). In the current study, we found that the Slits and Robos are necessary for the proper trajectory of the mdDA axon population through the diencephalon. Our results indicate that Slit/Robo signaling guides pioneer mdDA axons through the forebrain during their initial projection, defines the position of the tract, and prevents ectopic projections into the floor plate and other inappropriate midbrain and forebrain tissues.

Our strategy of examining the earliest stages of mdDA outgrowth showed widespread errors, more dramatic than predicted from the errant fibers observed in late embryonic brain tissue (Bagri et al., 2002). For example, we observed projections into ventral tissue, consistent with the ventral axon bundles seen at E18 (Bagri et al., 2002), but the early fibers also showed distinct abnormalities such as widening of the tract, dorsal errors, and errors in anterior diencephalon. The potential advantages of examining early embryos with whole mount antibody labeling included higher sensitivity which allowed the trajectories of individual axons to be visualized. It is also possible that some of the early errors that we identified are later pruned or corrected. Because homozygous mutations in Slit1/2 and Robo1/2 cause lethality at birth, the functional consequences of mdDA errors remain unknown. It seems likely that severe defects in the mdDA system would result from depleting the projections to normal targets, and additionally if misguided TH axons survive and make abnormal connections. We have observed that TH expression appears to be downregulated in some axonal populations after their initial projections are complete, such as the A13 population (Nural and Mastick, 2004), so not all early TH+ fibers maintain their TH expression.

4.1. Slit2, and not Slit1, is essential for directing mdDA projections into the MFB tract

Although both Slits are expressed in close proximity to the mdDA population, we found that Slit2 plays a dominant role in directing these axons into the MFB tract. Loss of the *Slit1* gene does not affect the course of the mdDA neurons as long as there is at least one wildtype *Slit2* allele. Conversely, removing only *Slit2* function, while retaining both *Slit1* alleles, results in invasion of the midline, including a characteristic ventral looping trajectory. In the $Slit1^{-/-}$; $Slit2^{-/-}$ double mutants, this looping phenotype is more disorganized and axons begin to wander dorsally. Expression of Slit2 along the ventral midline thus has a main function of keeping axons out of the ventral forebrain and floor plate. A stronger Slit2 function was similarly implicated by the pattern of defects seen in descending longitudinal tracts (Farmer et al., 2008). However, subsets of both descending and ascending axons show an additional phenotype of dorsal wandering, paradoxically away from the strong ventral midline source of Slit expression. Patches of dorsal tissue do express low levels of Slits, as detected by in situ hybridization, and might present a dorsal constraint to axon trajectories. Alternatively, Slits may have a specific function in promoting straight growth of longitudinal axons. Positive functions of Slits have been identified in previous studies, including that Slit2-N, the N-terminal fragment of Slit2, can promote elongation in some neuron populations (Nguyen Ba-Charvet et al., 2001; Wang et al., 1999).

4.2. Robos guide mdDA axons, in part through a Slit-independent function of Robo1

Most of the mutant phenotypes exhibited in the $Slit1^{-/-}$; $Slit2^{-/-}$ double mutants are also seen in $Robo1^{-/-}$; $Robo2^{-/-}$ double mutants. There is invasion of the ventral midline, dorsal wandering, and truncated axons. These shared phenotypes were expected, since Slits are the only known ligands for Robos. However, the disorganization of the mdDA projections was

more pronounced in *Robo1*$^{-/-}$; *Robo2*$^{-/-}$ mutants. Specifically, the dorsal wandering in *Robo1*$^{-/-}$; *Robo2*$^{-/-}$ double mutants was exaggerated with axons projecting as far as the dorsal midline and fasciculating along specific aberrant dorsal trajectories. An intriguing observation is that the ectopic dorsal tract appears to form at the same position as the small TH+ population of the mesohabenular pathway (described in Torre et al., 2010), so one possibility is that the ectopic tract in Robo mutants represents an increase in mesohabenular projections, or a precocious development of this pathway. Mesohabenular axons fail to project in Neuropilin-2 mutant mice (Torre et al., 2010), implying that this population of TH + axons use Npn2 and Robo1/2 receptors in opposing roles in their guidance (see further discussion below).

The increased wandering implies a partial Slit-independent function of Robo1 and 2, most obviously in the ectopic dorsal tract that was only seen in *Robo1*$^{-/-}$ and *Robo1*$^{-/-}$; *Robo2*$^{-/-}$ double mutants. Dorsal axon projections were unexpected. Given the strong ventral Slit expression, the prediction would be that axons lacking Robos would ignore this repellent signal and project toward the midline. In fact, Robo receptors appear to have a general Slit-independent role in preventing longitudinal axons from wandering dorsally. In a previous study, analysis of descending axon tracts of the midbrain and hindbrain revealed more severe phenotypes in *Robo1*$^{-/-}$; *Robo2*$^{-/-}$ double mutants when compared to *Slit1*$^{-/-}$; *Slit2*$^{-/-}$ double mutants, including more midline crossing and dorsoventral wandering, and extensive dorsal projections (Farmer et al., 2008).

Robos could have other unknown ligands. Alternatively, Robos may act as homophilic binding molecules (Liu et al., 2004; Sundaresan et al., 2004), and thus promote coherent tracts. Supporting this, Robos can work as cell-adhesion molecules promoting axonal outgrowth in vitro (Hivert et al., 2002), and the cytoplasmic domains of *Drosophila* Robo1 and Robo2 can dimerize in vitro (Simpson et al., 2000). In zebra fish, the longitudinal TPOC axons are dependent on interactions between Robo isoforms, possibly by modulating axon-axon adhesion (Divine and Key, 2008). Similarly, Robos may promote mdDA axon fasciculation into tightly organized tracts, independently of Slits. It must also be considered that mdDA axons are not pioneers, but project into an environment where they likely interact with and possibly fasciculate with pre-existing tracts (Figure 1). As earlier tracts may also be dependent on Slit/Robo guidance (Marion et al., 2005; Tsuchiya et al., 2009), mdDA errors may be a secondary consequence of the earlier tract errors. Defining the molecular pathways between Slit/Robo signals, other associated downstream signaling proteins, and interactions between axon populations will be an important part for understanding Slit/Robo roles in longitudinal axons.

Finally, from the perspective of mdDA projections, Robo2 appears largely redundant to Robo1, since *Robo2*$^{-/-}$ projections are normal. However, the fact that *Robo1*$^{-/-}$; *Robo2*$^{-/-}$ mutants are more severe than *Robo1*$^{-/-}$ mutants suggests that Robo2 can partially compensate for Robo1 loss, while not participating under normal circumstances.

4.3. The mdDA tract is established by the coordinated action of multiple cues

A comparison of several studies suggests that multiple cues collaborate to guide dopaminergic axons into a narrow ascending tract through the diencephalon. Their initial projections immediately turn anterior. Anterior directionality is partially determined by repulsion from a posterior source of Semaphorin, as a subset of mdDA axons grow posteriorly in Neuropilin2 (Nrp2) mutants (Yamauchi et al., 2009). Because prior studies showed that ventral tissue contained an local directionality for mdDA axons, which could be fully reversed by surgical rotation of patches of tissue (Nakamura et al., 2000), Semaphorin signals may represent one graded molecular component within the substrate tissue. Other unknown signals must also help contribute to directionality, because only a subset of axons

grows caudally in Neuropilin2 mutants. Anterior growth through the diencephalon is reduced in Sema3F mutants, which implicates a repellent gradient of Sema3F (Kolk et al., 2009). Once growth begins anteriorly, mdDA axons are highly restricted to a narrow path. This narrow path appears to result from multiple signals that keep axons from diverging ventrally or dorsally. The ventral boundary of the tract requires Slit/Robo signals, as Slit or Robo mutations result in many axons diverting ventrally (Bagri et al., 2002; this study). Interestingly, the dorsal limit to the tract depends on both Slit/Robo and Sema/Nrp2 signaling, as mutants for either pathway have similar errors of a subset of axons that stray dorsally (Kolk et al., 2009; Yamauchi et al., 2009), although dorsal spreading was not confirmed in another study of Nrp2 mutants (Torre et al., 2010). The dorsal Sema barrier likely arises from a midlateral arc of Sema3F expression in the midbrain and diencephalon (Hernandez-Montiel et al., 2008; Kolk et al., 2009; Yamauchi et al., 2009). However, the mechanism by which Slit/Robo signals prevent dorsal wandering is less obvious because little Slit expression is apparent in dorsal tissue. These negative signals are likely balanced by chemoattractive activities within the diencephalon, specifically ventral midline tissue expressing Netrin1 and Shh. Both of these signals are attractive for cultured mdDA axons (Hammond et al., 2009; Lin et al., 2005), and Shh receptor components are expressed in mdDA axons (Hammond et al., 2009). Netrin-1 expression is found in the ventral-lateral hypothalamic regions (Deiner and Sretavan, 1999), which roughly corresponds to the main ventral target of aberrant projections in Slit/Robo mutants. Additional Netrin expression has been observed along the ventral midline of the midbrain and forebrain (Livesey and Hunt, 1997). DCC, a Netrin-1 receptor involved in attractive signaling, is highly expressed by mdDA axons and is involved in the organization of the dopaminergic pathways (Flores et al., 2005). Furthermore, mdDA neurons are sensitive to Netrin-1 in vitro (Lin et al., 2005) and orient toward ectopic Netrin-1 in vivo (Vitalis et al., 2000). The potential chemoattractive responses of mdDA axons in the absence of Slit/Robo signaling suggests that these axons are capable of responding to both attractive and repulsive signals simultaneously. Presumably, such opposing signals would result in a push/pull mechanism, defining a precise ventrolateral trajectory through the diencephalon. Determining if mdDA and other axon populations can respond to opposing signals simultaneously will be an important step to understanding their guidance mechanisms. A final informative phenotype was that mdDA axons deviated from the MFB tract near the telencephalon to project anteriorly toward the optic stalk. Slit2 is known to be expressed around the optic chiasm and Slit1 around the optic stalk (Erskine et al., 2000). This anterior Slit expression may be important for the dorsal exit of mdDA axons from the diencephalon into the telencephalon. Finally, mdDA projections into the basal forebrain and cortex are less well defined, but include a surprising switch to become attracted to Semaphorin signals in the cortex (Kolk et al., 2009). Taken together, these studies suggest that even the simple initial mdDA projections through the diencephalon involve the collaboration of several guidance cues in the environment, as well as several types of receptors to mediate axonal responses.

4.4. Conclusions: Slit/Robo roles in the development and regeneration of the nigrostriatal pathway

The degeneration of the nigrostriatal pathway is the hallmark pathological feature associated with Parkinson's disease. Therapies being considered include transplanting fetal (or stem cell-derived) ventral mesencephalon dopaminergic neurons to restore the disrupted dopamine pathway (for a review, see Lindvall and Björklund, 2004). A challenge for effective transplant therapies is to what degree grafted dopaminergic axons will be able to grow out along appropriate pathways to find their targets. Understanding how dopaminergic axons navigate through their native environment may contribute to increasing efficiency and success in transplantations. Our experiments show that Slit/Robo signaling plays a crucial role in navigation of mdDA axonal projections, and provides an example of Slit/Robo

guidance of ascending longitudinal axons. A major influence is to keep axons out of the ventral midline, and thus projecting ipsilaterally, which matches the conventional role of Slits as midline repellents. An additional influence on longitudinal axons is in positioning them in a specific longitudinal tract. This lateral positioning role suggests novel Slit/Robo and Robo-specific roles in promoting longitudinal axons to grow straight. Continued study of these and other axon guidance molecules that contribute to proper navigation of the individual midbrain dopaminergic populations from the ventral mesencephalon to the striatum, basal forebrain, and cortex could provide information necessary for clinical therapy.

Acknowledgments

The *Robo* and *Slit* mutant founder mice, and probe DNAs, were gifts of Marc Tessier-Lavigne (Stanford; Genentech). We thank Elke Stein (Yale) for the gift of Robo antibodies. Several people in the Mastick lab provided help and discussions on this project, including Amy Altick, Sam McMahon, Brielle Bjorke, and Farnaz Shoja-Taheri. Min Kyung Kim helped with confocal imaging. We thank Tom Kidd and Chris von Bartheld for insights and helpful comments. We thank Claudia Garcia Pena (UNAM) for insights and advice. Use of the Nevada Genomics Center was supported by P20 RR-016464 from INBRE (NCRR). This projected was supported by the March of Dimes grant #1-FY06-387, and NIH grants HD38069 and NS054740 to GSM. The funding agencies had no role in producing this report.

References

Bagri A, Marin O, Plump AS, Mak J, Pleasure SJ, Rubenstein JL, Tessier-Lavigne M. Slit proteins prevent midline crossing and determine the dorsoventral position of major axonal pathways in the mammalian forebrain. Neuron 2002;33:233–248. [PubMed: 11804571]

Deiner MS, Sretavan DW. Altered midline axon pathways and ectopic neurons in the developing hypothalamus of netrin-1- and DCC-deficient mice. J Neurosci 1999;19:9900–9912. [PubMed: 10559399]

Devine CA, Key B. Robo-Slit interactions regulate longitudinal axon pathfinding in the embryonic vertebrate brain. Dev Biol 2008;313:371–383. [PubMed: 18061159]

Dickson BJ, Gilestro GF. Regulation of commissural axon pathfinding by slit and its Robo receptors. Annu Rev Cell Dev Biol 2006;22:651–675. [PubMed: 17029581]

Erskine L, Williams SE, Brose K, Kidd T, Rachel RA, Goodman CS, Tessier-Lavigne M, Mason CA. Retinal ganglion cell axon guidance in the mouse optic chiasm: expression and function of robos and slits. J Neurosci 2000;20:4975–4982. [PubMed: 10864955]

Farmer WT, Altick AL, Nural HF, Dugan JP, Kidd T, Charron F, Mastick GS. Pioneer longitudinal axons navigate using floor plate and Slit/Robo signals. Development 2008;135:3643–3653. [PubMed: 18842816]

Flores C, Manitt C, Rodaros D, Thompson KM, Rajabi H, Luk KC, Tritsch NX, Sadikot AF, Stewart J, Kennedy TE. Netrin receptor deficient mice exhibit functional reorganization of dopaminergic systems and do not sensitize to amphetamine. Molecular Psychiatry 2005;10:606–612. [PubMed: 15534618]

Grieshammer U, Ma L, Plump AS, Wang F, Tessier-Lavigne M, Martin1 GR. SLIT2-Mediated ROBO2 Signaling Restricts Kidney Induction to a Single Site. Developmental Cell 2004;6:709–717. [PubMed: 15130495]

Hammond R, Blaess S, Abeliovich A. Sonic hedgehog is a chemoattractant for midbrain dopaminergic axons. PLoS ONE 2009;4:e7007. [PubMed: 19774071]

Hernandez-Montiel HL, Tamariz E, Sandoval-Minero MT, Varela-Echavarria A. Semaphorins 3A, 3C, and 3F in mesencephalic dopaminergic axon pathfinding. J Comp Neurol 2008;506:387–397. [PubMed: 18041777]

Hivert B, Liu Z, Chuang CY, Doherty P, Sundaresan V. Robo1 and Robo2 are homophilic binding molecules that promote axonal growth. Mol Cell Neurosci 2002;21:534–545. [PubMed: 12504588]

Hu Z, Cooper M, Crockett DP, Zhou R. Differentiation of the midbrain dopaminergic pathways during mouse development. J Comp Neurol 2004;476:301–311. [PubMed: 15269972]

Kastenhuber E, Kern U, Bonkowsky JL, Chien CB, Driever W, Schweitzer J. Netrin-DCC, Robo-Slit, and heparan sulfate proteoglycans coordinate lateral positioning of longitudinal dopaminergic diencephalospinal axons. J Neurosci 2009;29:8914–8926. [PubMed: 19605629]

Kennedy TE, Serafini T, de la Torre JR, Tessier-Lavigne M. Netrins are diffusible chemotropic factors for commissural axons in the embryonic spinal cord. Cell 1994;78:425–435. [PubMed: 8062385]

Kolk SM, Gunput RA, Tran TS, van den Heuvel DM, Prasad AA, Hellemons AJ, Adolfs Y, Ginty DD, Kolodkin AL, Burbach JP, Smidt MP, Pasterkamp RJ. Semaphorin 3F is a bifunctional guidance cue for dopaminergic axons and controls their fasciculation, channeling, rostral growth, and intracortical targeting. J Neurosci 2009;29:12542–12557. [PubMed: 19812329]

Lin L, Rao Y, Isacson O. Netrin-1 and slit-2 regulate and direct neurite growth of ventral midbrain dopaminergic neurons. Mol Cell Neurosci 2005;28:547–555. [PubMed: 15737744]

Lindvall O, Björklund A. Cell therapy in Parkinson's disease. NeuroRx 2004;1:382–393. [PubMed: 15717042]

Liu Z, Patel K, Schmidt H, Andrews W, Pini A, Sundaresan V. Extracellular Ig domains 1 and 2 of Robo are important for ligand (Slit) binding. Mol Cell Neurosci 2004;26:232–240. [PubMed: 15207848]

Livesey FJ, Hunt SP. Netrin and Netrin Receptor Expression in the Embryonic Mammalian Nervous System Suggests Roles in Retinal, Striatal, Nigral, and Cerebellar Development. Mol Cell Neurosci 1997;8:417–429. [PubMed: 9143559]

Long H, Sabatier C, Ma L, Plump A, Yuan W, Ornitz DM, Tamada A, Murakami F, Goodman CS, Tessier-Lavigne M. Conserved roles for Slit and Robo proteins in midline commissural axon guidance. Neuron 2004;42:213–223. [PubMed: 15091338]

Lopez-Bendito G, Flames N, Ma L, Fouquet C, Di Meglio T, Chedotal A, Tessier-Lavigne M, Marin O. Robo1 and Robo2 cooperate to control the guidance of major axonal tracts in the mammalian forebrain. J Neurosci 2007;27:3395–3407. [PubMed: 17392456]

Marion JF, Yang C, Caqueret A, Boucher F, Michaud JL. Sim1 and Sim2 are required for the correct targeting of mammillary body axons. Development 2005;132:5527–5537. [PubMed: 16291793]

Mastick GS, Davis NM, Andrew GL, Easter SS Jr. Pax-6 functions in boundary formation and axon guidance in the embryonic mouse forebrain. Development 1997;124:1985–1997. [PubMed: 9169845]

Meijering E, Jacob M, Sarria J-CF, Steiner P, H. Hirling MU. Design and Validation of a Tool for Neurite Tracing and Analysis in Fluorescence Microscopy Images. Cytometry 2004;58A:167–176. [PubMed: 15057970]

Nakamura S, Ito Y, Shirasaki R, Murakami F. Local directional cues control growth polarity of dopaminergic axons along the rostrocaudal axis. J Neurosci 2000;20:4112–4119. [PubMed: 10818146]

Negoescu A, Labat-Moleur F, Lorimier P, Lamarcq L, Guillermet C, Chambaz E, Brambilla E. F(ab) secondary antibodies: a general method for double immunolabeling with primary antisera from the same species. Efficiency control by chemiluminescence. J Histochem Cytochem 1994;42:433–437. [PubMed: 7508473]

Nguyen Ba-Charvet KT, Brose K, Ma L, Wang KH, Marillat V, Sotelo C, Tessier-Lavigne M, Chedotal A. Diversity and specificity of actions of Slit2 proteolytic fragments in axon guidance. J Neurosci 2001;21:4281–4289. [PubMed: 11404413]

Nural HF, Mastick GS. Pax6 guides a relay of pioneer longitudinal axons in the embryonic mouse forebrain. J Comp Neurol 2004;479:399–409. [PubMed: 15514979]

Nural HF, Todd Farmer W, Mastick GS. The Slit receptor Robo1 is predominantly expressed via the Dutt1 alternative promoter in pioneer neurons in the embryonic mouse brain and spinal cord. Gene Expression Patterns 2007;7:837–845. [PubMed: 17826360]

Plump AS, Erskine L, Sabatier C, Brose K, Epstein CJ, Goodman CS, Mason CA, Tessier-Lavigne M. Slit1 and Slit2 cooperate to prevent premature midline crossing of retinal axons in the mouse visual system. Neuron 2002;33:219–232. [PubMed: 11804570]

Poirier LJ, Sourkes TL. Influence of the substantia nigra on the catecholamine content of the striatum. Brain 1965;88:1236–1239.

Sang Q, Wu J, Rao Y, Hsueh YP, Tan SS. Slit promotes branching and elongation of neurites of interneurons but not projection neurons from the developing telencephalon. Mol Cell Neurosci 2002;21:250–265. [PubMed: 12401446]

Savitt JM, Dawson VL, Dawson TM. Diagnosis and treatment of Parkinson disease: molecules to medicine. J Clin Invest 2006;116:1744–1754. [PubMed: 16823471]

Sesack S, Carr D. Selective prefrontal cortex inputs to dopamine cells: implications for schizophrenia. Physiology and behavior 2002;77:513–517. [PubMed: 12526992]

Simpson JH, Bland KS, Fetter RD, Goodman CS. Short-range and long-range guidance by Slit and its Robo receptors: a combinatorial code of Robo receptors controls lateral position. Cell 2000;103:1019–1032. [PubMed: 11163179]

Sundaresan V, Mambetisaeva E, Andrews W, Annan A, Knoll B, Tear G, Bannister L. Dynamic expression patterns of Robo (Robo1 and Robo2) in the developing murine central nervous system. J Comp Neurol 2004;468:467–481. [PubMed: 14689480]

Tessier-Lavigne M, Goodman CS. The molecular biology of axon guidance. Science 1996;274:1123–1133. [PubMed: 8895455]

Torre ER, Gutekunst CA, Gross RE. Expression by midbrain dopamine neurons of Sema3A and 3F receptors is associated with chemorepulsion in vitro but a mild in vivo phenotype. Mol Cell Neurosci 2010;44:135–153. [PubMed: 20298787]

Tsuchiya R, Takahashi K, Liu FC, Takahashi H. Aberrant axonal projections from mammillary bodies in Pax6 mutant mice: possible roles of Netrin-1 and Slit 2 in mammillary projections. J Neurosci Res 2009;87:1620–1633. [PubMed: 19115401]

Vitalis T, Cases O, Engelkamp D, Verney C, Price DJ. Defects of tyrosine hydroxylase-immunoreactive neurons in the brains of mice lacking the transcription factor pax6 [In Process Citation]. J Neurosci 2000;20:6501–6516. [PubMed: 10964956]

Voorn P, Kalsbeek A, B BJ-B, Groenewegen H. The pre- and postnatal development of the dopaminergic cell group in the ventral mesencephalon and the dopaminergic innervation of the striatum of the rat. Neuroscience 1988;25:857–887. [PubMed: 3405431]

Wang KH, Brose K, Arnott D, Kidd T, Goodman CS, Henzel W, Tessier-Lavigne M. Biochemical purification of a mammalian slit protein as a positive regulator of sensory axon elongation and branching. Cell 1999;96:771–784. [PubMed: 10102266]

Yamauchi K, Mizushima S, Tamada A, Yamamoto N, Takashima S, Murakami F. FGF8 signaling regulates growth of midbrain dopaminergic axons by inducing semaphorin 3F. J Neurosci 2009;29:4044–4055. [PubMed: 19339600]

Yuan W, Zhou L, Chen JH, Wu JY, Rao Y, Ornitz DM. The mouse SLIT family: secreted ligands for ROBO expressed in patterns that suggest a role in morphogenesis and axon guidance. Dev Biol 1999;212:290–306. [PubMed: 10433822]

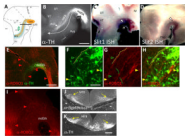

Figure 1.

TH+ axons project adjacent to Slit+ tissue, and express Robo1 and 2. A. Schematic representation of the initial mdDA projections through the diencephalon. The nucleus of the mdDA neurons is positioned along the cephalic flexure and extends across the forebrain/midbrain boundary. These TH+ axons project anteriorly in a distinct ventrolateral position through the thalamus. Adjacent to the MFB tract, the A13 cell population serves as a landmark. Black lines marked E-F and G-H indicate section planes in those panels. B. Wild-type whole mount embryo in the CD-1 background immunolabeled with TH. The white arrow represents the normal trajectory of mdDA axons through the thalamus. The tract is labeled MFB. C. *Slit1* mRNA expression (purple) is localized around the cephalic flexure, with robust signal at the ventral midline (arrowhead). Fainter graded expression domains are visible in dorsal midbrain, and dorsal and ventral thalamus. D. *Slit2* expression is also seen along the ventral midline, overlapping with the expression of *Slit1*. Very faint expression is also found in the hypothalamus and lateral thalamus. E. Robo1 (red) and TH (green) antibody labeling of a sagittal section of an E12.5 embryo. Robo1 is expressed in an extensive set of longitudinal bundles (E) which transit the mdDA nucleus. F-H. High magnification views of a different section. Some TH cell bodies are Robo1+ (yellow arrowheads), while other TH+ cell bodies do not show detectable Robo1 labeling (green arrowheads). The dotted lines trace a few examples of TH+ axons, of which some are closely associated with Robo1+ bundles (yellow), while other TH+ axons are not (green). I. Robo2 antibody labeling of a sagittal section of an E12.5 embryo. While Robo2 label can be seen in longitudinal fibers in dorsal, anterior, and posterior regions, little to no Robo2 label can be seen in the area of the mdDA or the MFB. J, K. Adjacent tissue sections showing anti-β-galactosidase immunolabeling representing expression from a *Robo2*^{lacZ} allele (J), in comparison to TH in the MFB (K). Both markers label MFB fibers (yellow arrows). Abbreviations: cf, cephalic flexure; cv, cerebral vesicle; DT, dorsal thalamus; Hyp, hypothalamus; M, midbrain; md, mesodiencephalon; MFB, medial forebrain bundle; op, optic stalk; VT, ventral thalamus. Scale Bars: B and E, 400 μm; (applies to C, D, I); F, 50 μm; (applies to G, H); K, 100 μm (applies to J).

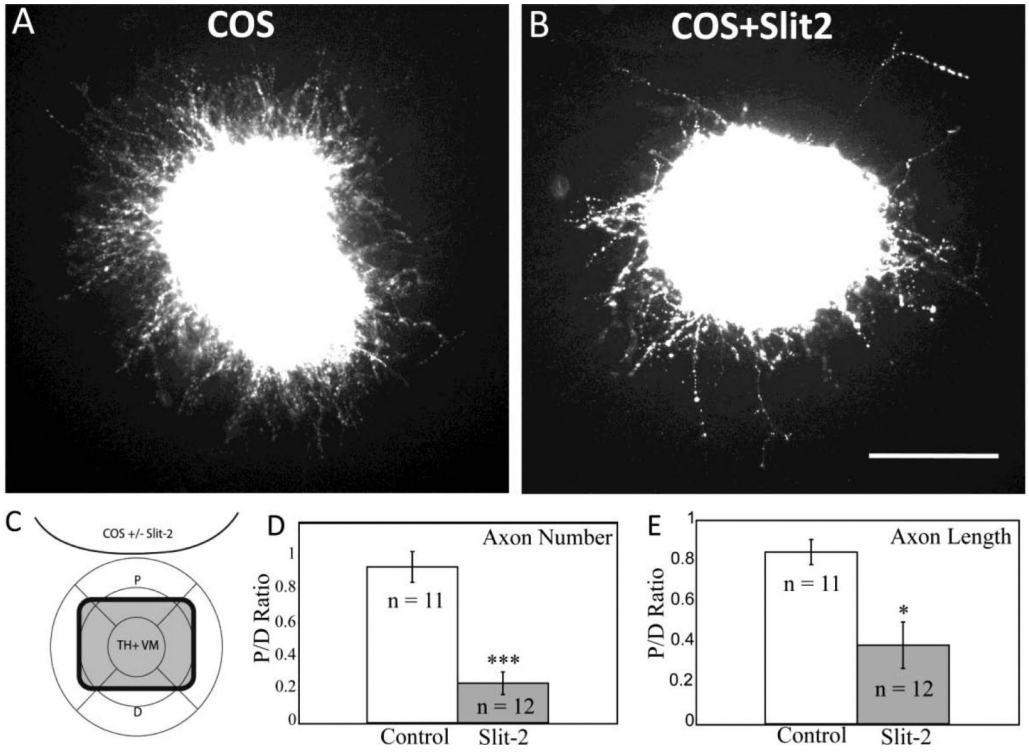

Figure 2.

TH+ axons are inhibited by secreted Slit2 in vitro. Ventral midbrain tissue from E12.5 mouse embryos was cultured for two days in collagen gel with aggregates of COS cells, followed by fixation and labeling with TH antibodies. Images are oriented with COS aggregates at the top. A. Control explant with mock-transfected COS cell aggregate. B. Explant challenged with Slit2-expressing COS cell aggregate. C. Schematic depicting TH+ ventral mesencephalic (VM) explant and COS cell aggregate (with or without Slit2 expression). Crosshairs define proximal (P) and distal (D) quadrants with relation to aggregate. Number and length of axons were determined in each quadrant and the ratio P/D was determined for every explant. D. P/D ratio of the number of axons in control explants versus explants cocultured with Slit2 expressing COS cells. E. P/D ratio of the length of axons in control explants versus explants cocultured with Slit2 expressing COS cells. The P/D ratio with Slit2 was significantly decreased compared to control explants, by t-test. ***p<.0001, *p<.05. Scale bar: 100 μm.

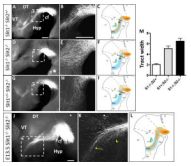

Figure 3.

Slits organize mdDA projections through the diencephalon, with a dominant role for Slit2. Whole-mount TH immunolabeling and schematics of E12.5 (A-I) and E13.5 (J-M) embryos at low (A,D,G,J) and high (B,E,H,K) magnification. A-C. TH+ axons in *Slit1*$^{-/-}$;*Slit2*$^{+/-}$ double mutants, with projections identical to wildtype controls (compare to Fig 1B). Note that TH+ axons project in an organized and relatively narrow ascending trajectory through the diencephalon toward the telencephalon. Axons avoid the ventral hypothalamus, and project ventral to the A13 landmark. D-F. *Slit1*$^{-/-}$; *Slit2*$^{-/-}$ double homozygotes form a wider tract, with many axons growing within ventral midline tissue near the cephalic flexure (E). In addition, axons have shorter projections with few in the proper direction, and some wandering dorsally. G-I. *Slit1*$^{+/+}$; *Slit2*$^{-/-}$ single mutant embryos are similar to *Slit1*$^{-/-}$; *Slit2*$^{-/-}$ double mutants, with projections looping into the ventral midline (*), extending over a wider dorsoventral breadth, and of shorter length than in control embryos. J-L. By E13.5 the ventral looping into the midline is still prevalent and mdDA neurons continue to project over a wider dorsoventral breadth, invading ventral midline tissue. K. Within the anterior diencephalon, mdDA axons deviate from the tract to project toward the optic stalk (arrow). Axons in the tract converge abnormally (arrowhead). M. Quantitation of the width of the mdDA tract, measured at the point indicated in the schematic summary of each mutant phenotype. Tract width is indicated by arbitrary units consistent between the genotype pools, +/- SEM. *Slit1*$^{-/-}$; *Slit2*$^{+}$ is a pool of control embryos (n=8) derived from the breeding stock of Slit1 homozygotes, with or without a *Slit2*$^{-}$ allele. *Slit1*$^{+}$; *Slit2*$^{-/-}$ are a similar pool of embryos with at least one *Slit1*$^{+}$ allele (n=6), compared to *Slit1*$^{-/-}$; *Slit2*$^{-/-}$ double mutants (n=7). By ANOVA, the three pools were significantly different. cf, cephalic flexure; DT, dorsal thalamus; Hyp, hypothalamus; M, midbrain; VT, ventral thalamus. Scale bars, in A and B represent 400 μm for low and high magnification, respectively.

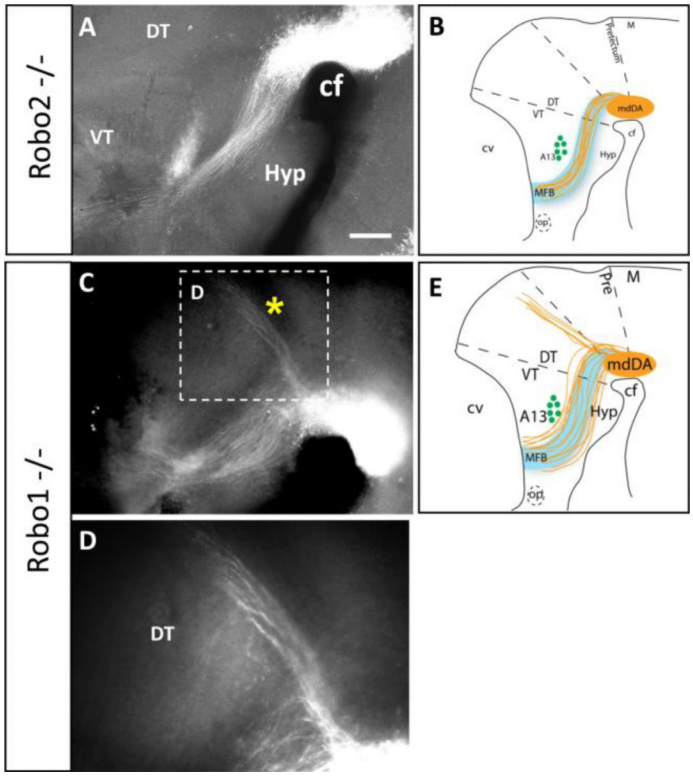

Figure 4.

Robo single mutants suggest a dominant role for *Robo1* in mdDA axon guidance. Whole-mount TH immunolabeling of E13.5 embryos shows *Robo2*$^{-/-}$ mutant (A) and *Robo1*$^{-/-}$ mutant phenotypes at low (A,C) and high magnification (D). A. *Robo2*$^{-/-}$ mutant embryos have normal axonal projections forming a narrow tract through the diencephalon (compare to Fig. 1B). C-E. *Robo1*$^{-/-}$ mutants are characterized by a dorsoventral broadening of the tract. Most axons continue along the MFB projecting into the telencephalon. However, a pronounced bundle of axons projects from the mdDA nucleus dorsally along the dorsal thalamus-pretectum boundary (* in C, magnified in D), and continues to the dorsal midline. cf, cephalic flexure; DT, dorsal thalamus; Hyp, hypothalamus; M, midbrain; op, optic stalk; VT, ventral thalamus. Scale bar in A, 400 μm for A and C.

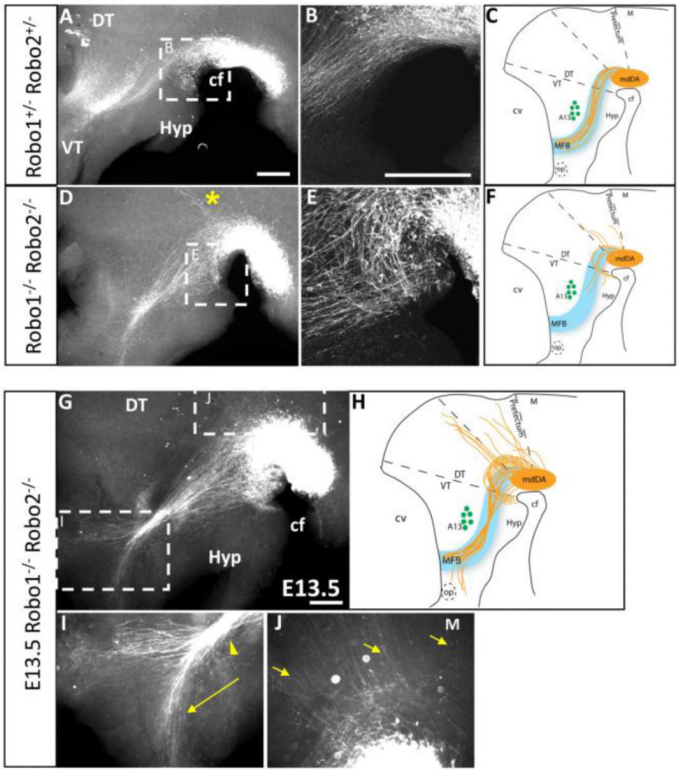

Figure 5.

Robo1 and 2 cooperate to guide mdDA axons through the diencephalon. Whole-mount TH immunolabeling of E12.5 (A-F) and E13.5 (G-J) embryos shows *Robo1/2* heterozygous (A-B) and double mutant (D-E, G-K) phenotypes at low (A,D,G) and high (B,E, I-K) magnification. A-C. *Robo1*$^{+/-}$; *Robo2*$^{+/-}$ embryos show a tract identical to wildtype controls. D-F. *Robo1*$^{-/-}$; *Robo2*$^{-/-}$double mutants are have axons growing toward and entering the ventral midline near the cephalic flexure, dorsoventral broadening of the tract, and shorter projections with few in the proper direction, identical to the *Slit1*$^{-/-}$; *Slit2*$^{-/-}$ double homozygous phenotype. Additionally, *Robo1*$^{-/-}$; *Robo2*$^{-/-}$ double mutants exhibit extensive dorsal wandering with axons fasciculating along aberrant trajectories (* in D). G-K. E13.5 *Robo1*$^{-/-}$; *Robo2*$^{-/-}$ double homozygotes have worsening errors, including dorsal wandering (J) and an anterior split in the tract, with some axons diverging anteriorly toward the optic stalk in the anterior forebrain (I). cf, cephalic flexure; DT, dorsal thalamus; Hyp, hypothalamus; M, midbrain; op, optic stalk; VT, ventral thalamus. Scale bars represent 400 μm.